

# Assessing progression or regression of CAD: The role of perfusion imaging

K. Lance Gould, MD

### **BENEFITS OF VIGOROUS RISK FACTOR TREATMENT**

Stabilization or regression of coronary atherosclerosis in response to vigorous risk factor treatment is well established by many trials based on clinical events and anatomic measurements of severity via coronary arteriography or intracoronary ultrasound. The reduction in coronary events is proportionately much greater than the small anatomic changes observed as a result of stabilization of plaques associated with decreased lipid content, inflammation, protease activity, and risk of plaque rupture. Thus small anatomic changes predict major corresponding changes in the risk of coronary events. Finally, more intense treatment is also associated with a lower risk of coronary events than casual treatment of risk factors.

However, the response to risk factor treatment is not predictable or consistent for individual patients. For example, statin monotherapy is associated with a 30% to 50% reduction in coronary events. Though significant for the general concept of treating risk factors, 50% to 70% of patients remain at risk of events. Combined multiple lipid active medications or intense lifestyle modification (or both) reduces the risk of coronary events by over 90% even for "secondary" management of established coronary artery disease (CAD).<sup>1-3</sup> Not everyone is willing or able to take multiple medications or adhere to a strict lifestyle regimen. For a specific patient, there is no way of knowing in advance what intensity of treatment will stabilize his or her vascular disease or whether it is progressing or stabilizing before an unexpected coronary event provides an answer in retrospect that is too late.

### **ARTERIOGRAPHIC CHANGES WITH LIPID LOWERING**

Although coronary arteriography and intracoronary ultrasound have documented regression of CAD in clinical trials, these invasive procedures are not justifiable for routine follow-up of medical treatment. Moreover, the anatomic changes measured by these technologies are so small, 0.1 to 0.3 mm, that large numbers of patients are required to determine the statistical significance of the changes because the variability of individual measurements is larger than the average change that becomes significant only for a large group. Consequently, even these invasive technologies do not provide a satisfactory guide to progression or regression for an individual in clinical practice. For objectively assessing quantitative changes in the severity of coronary atherosclerosis, they also require substantial experience and meticulous attention to technical details that are commonly not achieved in most clinical invasive laboratories despite being widely used and visually interpreted for diagnostic purposes.

For assessing diffuse coronary atherosclerosis, both of these invasive techniques are inadequate. For example, Hausmann et al<sup>4</sup> have demonstrated that in asymptomatic patients with risk factors, coronary arteriography entirely misses 70% of diffuse CAD compared with intracoronary ultrasound. On the other hand, intracoronary ultrasound does not provide an integrated measure of all of the changes throughout the coronary artery tree, where these changes are commonly heterogeneous with progression in one area and regression in another area in the same or different coronary arteries of an individual.

The importance of tracking the changes in CAD for an individual is illustrated in the myocardial perfusion images of Figure 1 by use of positron emission tomography (PET). (All PET images and software displays illustrated in this review were obtained with a Positron PET scanner [Positron Corp, Houston, TX]). This patient had successfully undertaken a vigorous healthy lifestyle regimen on low-fat food, achieving the ideal lean weight and regularly exercising, in addition to taking a statin, with a total cholesterol level of 148 mg/dL, a triglyceride level of 62 mg/dL, and low-density lipoprotein (LDL) and high-density lipoprotein (HDL) levels of 72 and 64 mg/dL, respectively, for 3 years after a normal baseline dipyridamole PET scan. However, the 3-year follow-up dipyridamole scan showed

From the Weatherhead PET Center, University of Texas Medical School, Houston, Tex.

Reprint requests: K. Lance Gould, MD, University of Texas Medical School, Weatherhead PET Center, Room 4.256 MSB, 6431 Fannin St, Houston, TX 77030.

J Nucl Cardiol 2005;12:625-38.

1071-3581/\$30.00

Copyright © 2005 by the American Society of Nuclear Cardiology.

doi:10.1016/j.nuclcard.2005.09.004

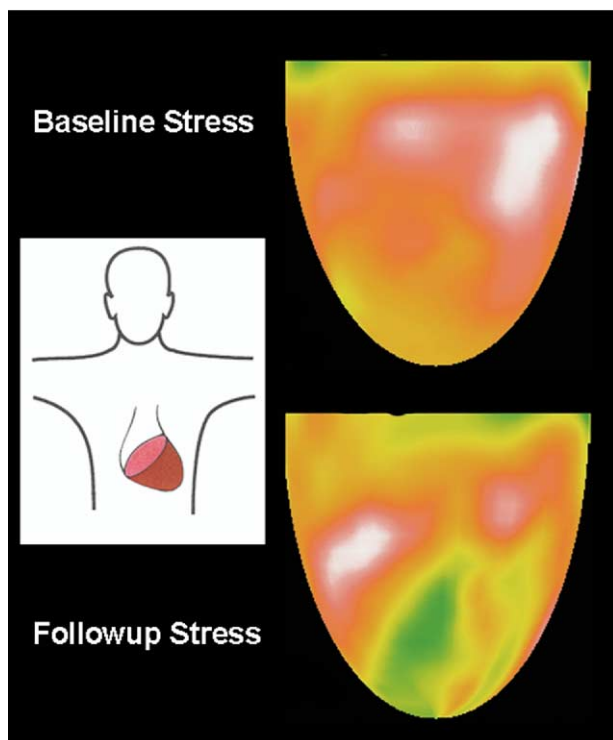


**Figure 1.** Myocardial perfusion images by PET after dipyridamole stress at baseline and at 3-year follow-up showing progression of CAD despite an excellent lifestyle and medical regimen, thereby leading to additional laboratory studies and treatment.

definite progression with a new perfusion defect despite an ideal regimen. On further evaluation to explain this unexpected progression, subfraction analysis of his lipid levels showed a lipoprotein (Lp[a]) of 149 mg/dL, which is 50 times the upper limit of normal (30 mg/dL) for that laboratory. Niaspan (Kos Pharmaceuticals, Inc, Miami, Fla) was then added (2000 mg daily), which would not have otherwise been used.

### COMPUTED TOMOGRAPHY AND MAGNETIC RESONANCE IMAGING WITH CORONARY ARTERIOGRAPHY

Magnetic resonance imaging (MRI) and computed tomography (CT) are currently being tested for assessing the anatomic severity of CAD by noninvasive coronary arteriography,<sup>5-9</sup> including changes in CAD in human beings.<sup>7</sup> However, there is great scatter in the quantitative correlation between invasive and noninvasive CT arteriography such that CT is not able to quantify stenosis severity because of inadequate resolution, coronary calcification, and several other technical problems.<sup>5,6,9</sup> Coronary calcium scores do not improve with lipid treatment.<sup>10</sup>

It is useful to put this problem of anatomic resolution

into perspective as the basis for understanding the value of perfusion imaging for following changes in CAD. The resolution requirement for experimental quantitative coronary arteriography adequate to predict fluid dynamic severity and corresponding changes in severity is well defined. The author first published the experimental validation of basic pressure-flow characteristics of stenosis, correlation with coronary flow reserve, and quantitative coronary arteriography of localized stenosis and of diffuse coronary disease.<sup>11-15</sup> The coronary arteriograms for the first series of these experimental studies used high-resolution, fine-grain, cut film and film cassettes; electrocardiography (ECG)-triggered intracoronary power injections of contrast medium; and a single diastolic frame triggered by ECG. The measured arteriographic resolution was 10 line pairs/mm in order to resolve lumen diameters to 0.1 mm, which is necessary for calculation of pressure-flow effects of stenosis in comparison to direct flowmeter measurements. Later experimental studies used cine arteriograms with a resolution of 4 line pairs/mm that resolves 0.25-mm-diameter dimensions for calculating coronary flow reserve in comparison to flowmeter measurements. A lower resolution is simply not adequate to predict the physiologic severity of stenosis or its changes.

The resolution of MRI and CT scanners is typically expressed in slice thickness or pixel dimensions. However, the many classical factors of physics still apply regarding signal strength, detector size, and the tradeoff of spatial versus density resolution. For the most advanced CT scanner (either 16 or 48 slices), the best measured resolution on a static idealized phantom is 1.2 line pairs/mm, as measured personally by the author with a physicist to confirm the results.

Because the detector sizes in the 16- and 64-slice CT scanners are the same, the spatial resolution is also the same. The 64-slice CT scanner covers a bigger field and is therefore "faster," with shorter exposure times and less motion blurring, but the spatial resolution is the same. An optimal, idealized resolution of 1.2 line pairs/mm means that 0.8 mm can be resolved at best under static idealized conditions. That resolution is not good enough to determine whether there are 0.1- to 0.3-mm changes in an individual stenosis in the range measured by invasive quantitative coronary arteriographic studies. In clinical practice, motion blurring, low-density contrast, scattered radiation, low signal-to-noise ratio, and other variables reduce the effective final resolution to less than the 0.8 mm resolvable on a static idealized phantom. Consequently, current noninvasive CT and MRI arteriograms cannot adequately quantify stenosis severity or its changes<sup>5,6,8,9</sup> because these technologies have only one third to one fourth of the effective resolution needed to approach the spatial resolution of invasive coronary

arteriography, which is itself limited for measuring changes in stenosis severity.

Plaque imaging is even more difficult because a major determinant of plaque instability is the thickness of the overlying fibrous cap that can be resolved now only by intracoronary ultrasound. Of course, CT and MRI technologies will be tested further for following changes in CAD despite these limitations. Even the author has obtained a GE 16-slice PET-CT scanner in addition to his Positron Corporation PET scanners (General Electric Healthcare, Waukesha, Wis) for studying these applications, particularly arteriographic enhancements for quantifying disease severity. However, this brief review of anatomic imaging and its limitations by one of the founders of quantitative coronary arteriography serves to highlight the role of noninvasive myocardial perfusion imaging as currently being more powerful than anatomic imaging for following changes in CAD.

### MYOCARDIAL PERFUSION FOR FOLLOWING CHANGES IN SEVERITY

Coronary blood flow is a function of the arterial radius raised to the fourth power. Therefore small changes in diameter not measurable by anatomic imaging are magnified into much larger changes in blood flow that are readily seen and quantifiable by perfusion imaging if done properly, free of artifacts that commonly affect both PET and single photon emission computed tomography imaging. For diffuse coronary atherosclerosis, a mild anatomic reduction in diameter that cannot be detected by visually interpreted arteriograms will cause cumulatively increasing resistance along the length of the coronary artery.<sup>15</sup> This cumulative resistance causes a base-to-apex longitudinal perfusion gradient by dipyridamole PET perfusion imaging that identifies diffuse disease.<sup>16</sup> It also causes a progressive graded pressure gradient along the artery toward that apex that is the pressure equivalent of the base-to-apex longitudinal perfusion gradient.<sup>17</sup>

What is the evidence showing that perfusion imaging is useful for following changes in coronary disease? Several studies using single photon stress perfusion imaging demonstrated improvement in patients undergoing risk factor treatment compared with control subjects.<sup>18-21</sup> PET perfusion imaging has also been developed specifically for following changes in CAD.<sup>3,22-25</sup> Myocardial perfusion abnormalities may show rapid improvement in within 40 to 90 days after intense risk factor treatment is started.<sup>22,24</sup>

In the Lifestyle Heart Trial, using endpoints of both PET perfusion images and quantitative coronary arteriography, the PET changes were proportionately greater with greater statistical significance than the changes in quantitative coronary arteriography.<sup>23</sup> We have also shown greater benefit on myocardial perfusion and cor-

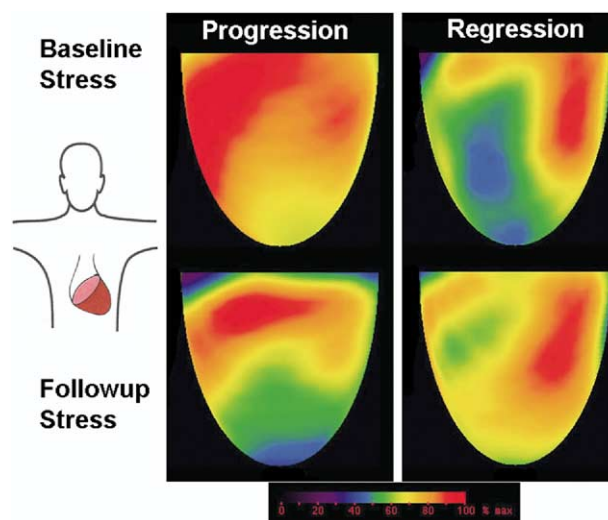
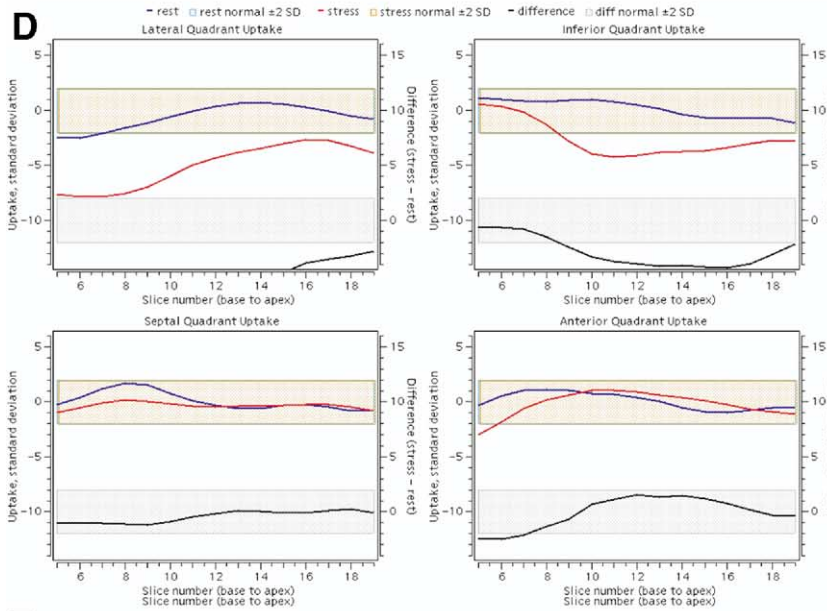
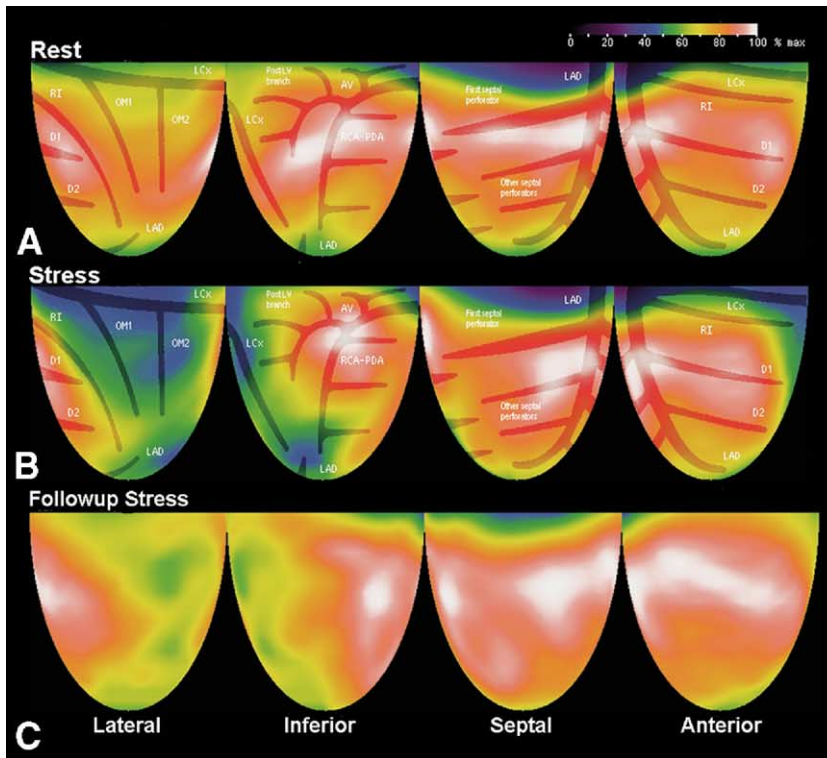


**Figure 2.** Myocardial perfusion images by PET after dipyridamole stress at baseline and at follow-up showing progression in a suboptimally treated patient and regression of CAD in another patient after an excellent lifestyle and medical regimen.

onary events with vigorous treatment to strict goals by combined pharmacologic and lifestyle management compared with the usual less rigorous or inadequate treatment.<sup>3</sup> Figure 2 demonstrates PET perfusion images of progression and regression of CAD in optimally versus suboptimally treated patients.

By use of severe disease as an example of quantifying changes, Figure 3 illustrates a normal resting perfusion scan (Figure 3A) and a severe stress-induced perfusion defect (Figure 3B), as well as its improvement 3 years later (Figure 3C) on a vigorous lifestyle regimen with 40 mg simvastatin to achieve a total cholesterol level of 134 mg/dL, triglyceride level of 68 mg/dL, LDL level of 68 mg/dL, HDL level of 52 mg/dL. The arterial overlay shows the arterial distributions corresponding to the perfusion map. Quantification of relative myocardial uptake for each quadrant of the heart (Figure 3D) in SD units shows the rest scan (blue line) within  $\pm 2$  SDs of 50 healthy control subjects (4 SDs within the blue shaded area). The stress uptake in SD units (red line) is well outside  $\pm 2$  SDs of normal limits (red shaded area). The printout of quantitative changes in the baseline to follow-up stress images (Figure 3E) shows improvement in all measures of severity as follows: (1) the size of the defect expressed as percent of the heart outside  $\pm 2$  SDs of normal decreased from 28.8% to 17.7% of the left ventricle, (2) the severity or relative activity expressed as percent of maximum counts improved from 53.5% to 71.3% of maximum activity, and (3) the combined size-severity expressed as the percent of the left ventricle with less than 60% of maximum counts improved from 30.8% to 2.1% of the left ventricle.

Figure 4 illustrates a milder stress-induced perfusion



	Patient	Normal Range	Mean ± SD
% of LV with Gradient < 2.0 SD (%)	Stress 1: 10.00	0.00 to 10.98	2.92 ± 8.06
Whole LV Gradient (SD units)	Stress 1: 0.00	0.00 to 7.18	1.20 ± 5.98
Worst Quadrant Gradient (SD units)	Stress 1: 0.00	0.00 to 1.12	0.30 ± 0.82
	Stress 2: 0.00	0.00 to 0.54	0.09 ± 0.45
% of LV with Uptake < 60% of max (%)	Stress 1: 2.81	0.00 to 1.73	0.68 ± 1.05
	Stress 2: 0.00	0.00 to 1.73	0.68 ± 1.05
% of LV with Uptake > 80% of max (%)	Stress 1: 30.81	0.63 to 9.37	5.00 ± 4.37
	Stress 2: 2.05	0.00 to 2.07	0.86 ± 1.21
% of LV with Ratio > 1.00 (%)	Stress 1: 34.68	36.10 to 69.30	52.70 ± 16.60
% of LV with Uptake < 2.5 SD (%)	Stress 1: 55.05	59.56 to 82.82	71.19 ± 11.63
Minimum Average Quadrant Activity (% of Max)	Relative Ratio: 84.06		
	Stress 1: 28.83	0.00 to 2.97	0.76 ± 2.21
	Stress 2: 17.66	0.00 to 2.27	0.72 ± 1.55
Homogeneity (no units)	Stress 1: 53.52	73.62 to 81.28	77.45 ± 3.83
	Stress 2: 71.34	79.57 to 85.11	82.34 ± 2.77
Homogeneity change (no units)	Stress 1: 0.48	0.44 to 0.66	0.55 ± 0.11
	Stress 2: 0.60	0.58 to 0.80	0.69 ± 0.11
	Stress 2 - Stress 1: 0.12		

defect (Figure 4A) improving after 3 years of vigorous lifestyle and pharmacologic treatment (Figure 4B), with overlays of the arterial regions as an optional display. Quantitative analysis (Figure 4C) shows the baseline stress (red dashed line) uptake outside  $\pm 2$  SDs of normal but uptake within these normal limits on the follow-up stress image (red solid line). The combined size-severity on the stress scans (percent of left ventricle with activity  $< 60\%$  of maximum activity) improved from 9.3% to 5.0% of the left ventricle.

As these examples illustrate, myocardial perfusion imaging for following changes in regional perfusion defects as a result of flow-limiting stenosis is scientifically well established and has demonstrated applicability in routine clinical practice but is used in only a few centers.

### TRADITIONAL INVASIVE MANAGEMENT OF CAD

In traditional management of CAD, a significant stress-induced perfusion defect leads to coronary arteriography and, commonly, a balloon angioplasty or stent, particularly given documented visual overestimation of stenosis severity. With the basic problem of attenuation artifacts and uncertain reliability of assessing disease severity by single photon emission computed tomography perfusion imaging, the invasive arteriogram is considered to provide the “hard definitive” clinical information.

On the other hand, revascularization procedures may be safely deferred for mild to moderate stenosis with a pressure-derived fractional flow reserve of 0.75 or greater, corresponding to a relative coronary flow reserve of 75% of normal,<sup>26,27</sup> which is, however, an invasive measurement. In addition, most plaque ruptures and coronary events occur at sites of diffuse atherosclerosis without prior significant stenosis,<sup>28</sup> where plaque rupture is prevented by aggressive risk factor treatment as first proposed by Brown<sup>29-31</sup> and documented by many subsequent lipid trials. Finally, active plaque inflammation with potential rupture is diffuse throughout the coronary artery tree, not located in a single “vulnerable” plaque,<sup>32</sup> thereby explaining in large part why

meta-analysis of revascularization procedures shows no survival benefit in stable CAD.<sup>33</sup>

These observations then become the basis for the next logical question for nuclear cardiology: Can artifact-free myocardial perfusion imaging provide unique definitive information for following the changes in CAD, as well as on early subclinical coronary atherosclerosis or its changes, even before flow-limiting stenoses that do not warrant invasive procedures appear?

The literature provides a positive answer, documenting that myocardial perfusion imaging without artifacts objectively and accurately (1) quantifies differences in relative regional perfusion of 10% or more corresponding to mild subclinical stenosis, (2) quantifies the base-to-apex longitudinal perfusion gradient of diffuse coronary atherosclerosis before significant flow-limiting stenosis occurs, and (3) quantifies the heterogeneity of resting myocardial perfusion and its changes after dipyridamole or adenosine as an index of endothelial dysfunction before significant flow-limiting stenosis occurs.

These 3 tasks can be accomplished for routine clinical purposes if the following criteria are met: (1) advanced, validated quantitative cardiac software specifically designed for objectively assessing quantitative changes in myocardial PET perfusion images; (2) perfusion images with uniform resting and stress images having less than 5% to 10% variation in regional relative radionuclide uptake in normal young volunteers having no risk factors; (3) capacity to quantify small regional differences of 10% or greater in patients with risk factors or mild subclinical CAD; and (4) no attenuation, misregistration, or other artifacts or suboptimal quality, all of which require compulsive attention to every technical detail, not commonly done in most PET laboratories.

### TECHNICAL IMAGING REQUIREMENTS

In the author’s experience, these technical requirements include over 12 million true coincidence counts per heart data set, or over 24 million total counts, because

---

**Figure 3.** For severe CAD, myocardial perfusion images by PET at rest (A) and after dipyridamole stress (B) at baseline and after dipyridamole stress at 3-year follow-up (C). On the baseline rest-stress images, the arterial overlay shows the affected arteries. Quantitative analysis of the baseline rest-stress images (D) graphs relative radionuclide uptake in SD units on the vertical axis for each base-to-apex tomographic slice on the horizontal axis for each quadrant of the heart. The shaded areas show  $\pm 2$  SD units or a 4-SD range of 50 healthy control subjects. Blue indicates the resting image, and red indicates the stress image. The black lines and shaded areas indicate the rest-to-stress change or  $\Delta$  of the rest-stress paired images. A printout of quantitative changes shows improvement in all measures of severity (E). RI, Ramus intermedius; OMI, first obtuse marginal branch; OM2, second obtuse marginal branch; LCx, left circumflex; D1, first diagonal branch; D2, second diagonal branch; LAD, left anterior descending; Post LV branch, posterior left ventricular branch; AV node branch, atrio-ventricular node branch, 1<sup>st</sup> Septal, first septal perforator branch; septals, septal perforator branches; RCA, right coronary artery; PDA, posterior descending artery.

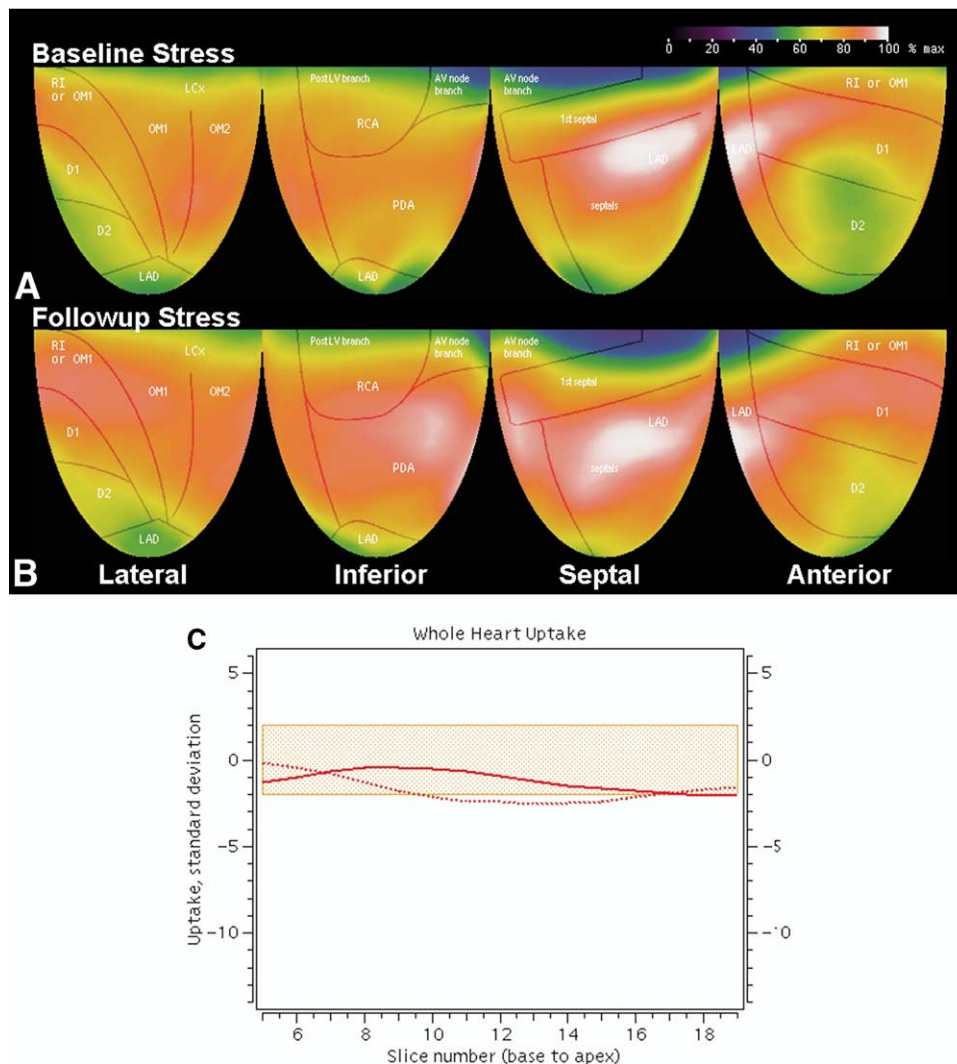


**Figure 4.** For mild CAD, the baseline stress images (A) show improvement compared with stress images (B) after 3 years of vigorous lifestyle and medical treatment. Arterial regions are overlaid on the perfusion maps. Quantitative comparison of the stress images (C) for the whole heart shows relative uptake in SD units improving from baseline (dashed line) to follow-up (solid line). The shaded area indicates  $\pm 2$  SDs of the stress images from 50 healthy control subjects. Red indicates that the two comparison studies are both during stress, whereas a rest-rest comparison would be in blue. RI, Ramus intermedius; OMI, first obtuse marginal branch; OM2, second obtuse marginal branch; LCx, left circumflex; D1, first diagonal branch; D2, second diagonal branch; LAD, left anterior descending; Post LV branch, posterior left ventricular branch; AV node branch, atrio-ventricular node branch, 1<sup>st</sup> Septal, first septal perforator branch; septals, septal perforator branches; RCA, right coronary artery; PDA, posterior descending artery.

approximately half of the counts are random coincidences. Our testing indicates that for either cardiac PET-CT with CT attenuation correction or standard PET with a rotating rod for attenuation correction, it is essential to use 2-dimensional imaging with extended septa, filtered backprojection, and early acquisition at 70 to 80 seconds after the start of infusion for adequate myocardial perfusion images by use of rubidium 82. It is important to check every image for correct coregistration of attenuation-emission images and to

correct shift artifacts, which occur in about 20% of all cardiac PET studies<sup>34</sup> with both types of scanners.

Thus the requirements for cardiac PET are substantially different than for cancer, brain, or whole-body PET. Cancer PET uses hot-spot imaging, where the background scatter and nonuniformity of 3-dimensional imaging and ordered-subsets expectation maximization reconstructions are not particularly important. However, for cold-spot imaging of mild defects for detecting early coronary ath-

erosclerosis or modest changes in severity, particularly with Rb-82, 2-dimensional acquisition with extended septa and filtered backprojection reconstruction are essential for adequate image quality.

Using these exacting technical standards, we have demonstrated (1) that the objectively measured quantitative severity of PET perfusion defects parallels stenosis severity by automated quantitative coronary arteriography<sup>35</sup> and precise anatomic location in the coronary artery tree even for small secondary branches,<sup>36</sup> (2) the theoretic basis for, the experimental validation of, and the clinical application of the base-to-apex longitudinal perfusion gradient for quantifying diffuse coronary narrowing before flow-limiting localized stenosis occurs,<sup>14-16</sup> and (3) heterogeneity of resting myocardial perfusion as a marker of coronary endothelial dysfunction as highly predictive of coronary atherosclerosis.<sup>37</sup> Because this latter concept is new but relevant for assessing preclinical coronary atherosclerosis by perfusion imaging, a brief review of experimental and human coronary endothelial function is appropriate.

### CORONARY ENDOTHELIAL FUNCTION

Coronary endothelial function includes a wide range of diverse vascular behavior in 3 interdependent categories—vasomotor control, platelet interactions/thrombosis, and cellular proliferation. Although imaging any of these processes is important, this discussion focuses on endothelial vasomotor function as a potential marker of early atherosclerosis before fully developed plaques associated with rupture, thrombosis, and clinical events appear.

Coronary endothelial function expressed as altered vasomotion has been assessed in human beings primarily by use of arteriography or intracoronary ultrasound to measure changes in arterial diameter or flow velocity before and after acetylcholine, arterial or arteriolar vasodilators, therapeutic interventions, or blocking agents such as  $N^G$ -monomethyl-L-arginine. Such studies have established our current understanding of endothelial function or dysfunction but are not necessarily useful for routine clinical practice.

Moreover, these techniques are invasive and provide primarily anatomic data or flow velocity of the epicardial coronary arteries. Whereas arterial flow velocity may reflect average downstream arteriolar behavior, the coronary endothelial dysfunction associated with atherosclerosis is heterogeneous both in epicardial coronary arteries and into the microvasculature.

Vascular mediators derived from coronary endothelium include prostacyclin, nitric oxide, thromboxane, endothelin, bradykinin, angiotensin, serotonin, substance P, C-type natriuretic peptide (an endothelium-derived hyperpolarizing factor), and others. The mechanisms affecting coronary vasomotion may be a complex balance be-

tween inhibition of normal vasodilatory mediators, such as nitric oxide, and activation of vasoconstrictor mediators, such as endothelin, and/or several other mediators acting simultaneously.

The stimuli, mediators, and vascular responses of epicardial coronary arteries and the coronary microvasculature are quite different, even divergent. For example, in the epicardial coronary arteries, acetylcholine-induced vasodilation is mediated by nitric oxide.<sup>38-40</sup> However, in the coronary microcirculation, acetylcholine-induced arteriolar vasodilation and increased coronary flow are not mediated by nitric oxide.<sup>41-43</sup> With epicardial artery endothelial dysfunction, acetylcholine causes arterial vasoconstriction whereas arteriolar vasodilation with increased flow remains intact as an example of divergent pathophysiologic behavior of the macrovasculature and microvasculature of the heart.<sup>38,41,44-46</sup>

As a further example, endothelial nitric oxide production mediates epicardial coronary artery vasodilation during exercise but is not involved in arteriolar vasodilation and increased coronary flow during exercise<sup>44</sup> unless there is a flow-limiting stenosis, where nitric oxide helps maintain perfusion during exercise.<sup>47</sup> In opposition to these vasodilator mechanisms, endothelin is a powerful coronary arteriolar vasoconstrictor that is activated in coronary atherosclerosis in parallel with inhibition of nitric oxide production.

Thus there is no single specific vasomotor abnormality, gold standard, diagnostic test, or even definition that identifies or defines coronary endothelial dysfunction. The hallmark of coronary endothelial dysfunction is mild heterogeneous vasoconstriction of coronary arteries or coronary microvasculature (or both) under a wide spectrum of different conditions, as well as vasomotor stimuli involving many different mechanisms including inhibition of vasodilator mechanisms or activation of vasoconstrictor mechanisms by many different interacting vasoactive mediators.

### HETEROGENEITY OF MYOCARDIAL PERFUSION AS CLINICAL MARKER

Heterogeneity of coronary endothelial function has been well documented in human beings<sup>48-50</sup> with associated altered coronary blood flow or perfusion reflecting coronary arteriolar dysfunction, as well as epicardial arterial endothelial dysfunction.<sup>51-55</sup> Resting coronary flow falls by approximately 20% after inhibition of coronary endothelial nitric oxide production without significant reduction in maximum coronary flow or coronary flow reserve,<sup>38,41,44-46</sup> thereby reflecting altered resting microvascular function.

Coronary endothelial dysfunction is closely associated with microvascular dysfunction of CAD or its risk factors,<sup>54-57</sup> may be familial as an independent risk factor,<sup>58</sup> and predicts future coronary events<sup>59-62</sup> or clinically man-

ifest disease up to 10 years later.<sup>62</sup> Cold pressor testing with measurements of coronary flow reserve involves complex sensory and efferent vasomotor control mechanisms separate from endothelial function with such great variability in normal subjects that its diagnostic utility is limited.<sup>63,64</sup>

Coronary flow reserve and myocardial perfusion imaging after pharmacologic arteriolar vasodilation for identifying flow-limiting coronary artery stenosis were first reported by the author<sup>65-68</sup> and are now in widespread use for routine diagnostic procedures. In this paradigm the resting perfusion image serves as a baseline for comparison to the stress perfusion image for identifying discrete regional perfusion abnormalities resulting from flow-limiting coronary artery stenosis, myocardial scar, or hibernating myocardium.

In contrast, we also first described resting perfusion defects that improve or disappear during pharmacologic stress, leaving a normal or improved stress image compared with the abnormal resting perfusion image, which we hypothesized was a result of endothelial dysfunction that reduces resting myocardial blood flow but not the response to these primarily direct smooth muscle vasodilators.<sup>69</sup>

In further research on this observation, we have recently reported a distinctly different diffuse patchy heterogeneity of resting myocardial perfusion as a marker of coronary endothelial dysfunction associated with coronary atherosclerosis separately, independently from and around these traditional discrete regional myocardial perfusion defects caused by flow-limiting stenosis or myocardial scar.<sup>37</sup> We used a mathematical technique from Markovian homogeneity analysis<sup>70</sup> to provide precise, objective, automated quantification of this resting perfusion heterogeneity in over 1000 patients and in 50 healthy normal reference subjects, demonstrating a basic new observation in myocardial perfusion imaging with potentially important clinical implications.

Patchy heterogeneous resting myocardial perfusion by noninvasive cardiac PET quantified objectively by use of Markovian homogeneity analysis and its improvement after dipyridamole are powerful independent predictors of even mild stress-induced perfusion abnormalities, more than standard risk factors, consistent with coronary microvascular dysfunction as an early marker of preclinical CAD for potential preventive treatment. The heterogeneity that we observe by PET perfusion imaging is macroscopic for the 1-cm<sup>3</sup> PET resolution in arterial distributions, separate from and unrelated to the dispersion of perfusion in small 1-mm myocardial samples used for microsphere measurements of perfusion in experimental animals.<sup>71,72</sup>

In view of the different, sometimes divergent arterial and arteriolar behaviors in response to the wide variety of vasoactive mediators, resting perfusion heterogeneity would not necessarily be expected to parallel the effects of intracoronary acetylcholine or cold pressor testing, just as

the arteriolar response to acetylcholine with increased blood flow does not parallel its vasoconstrictive effect on epicardial coronary arteries in CAD.

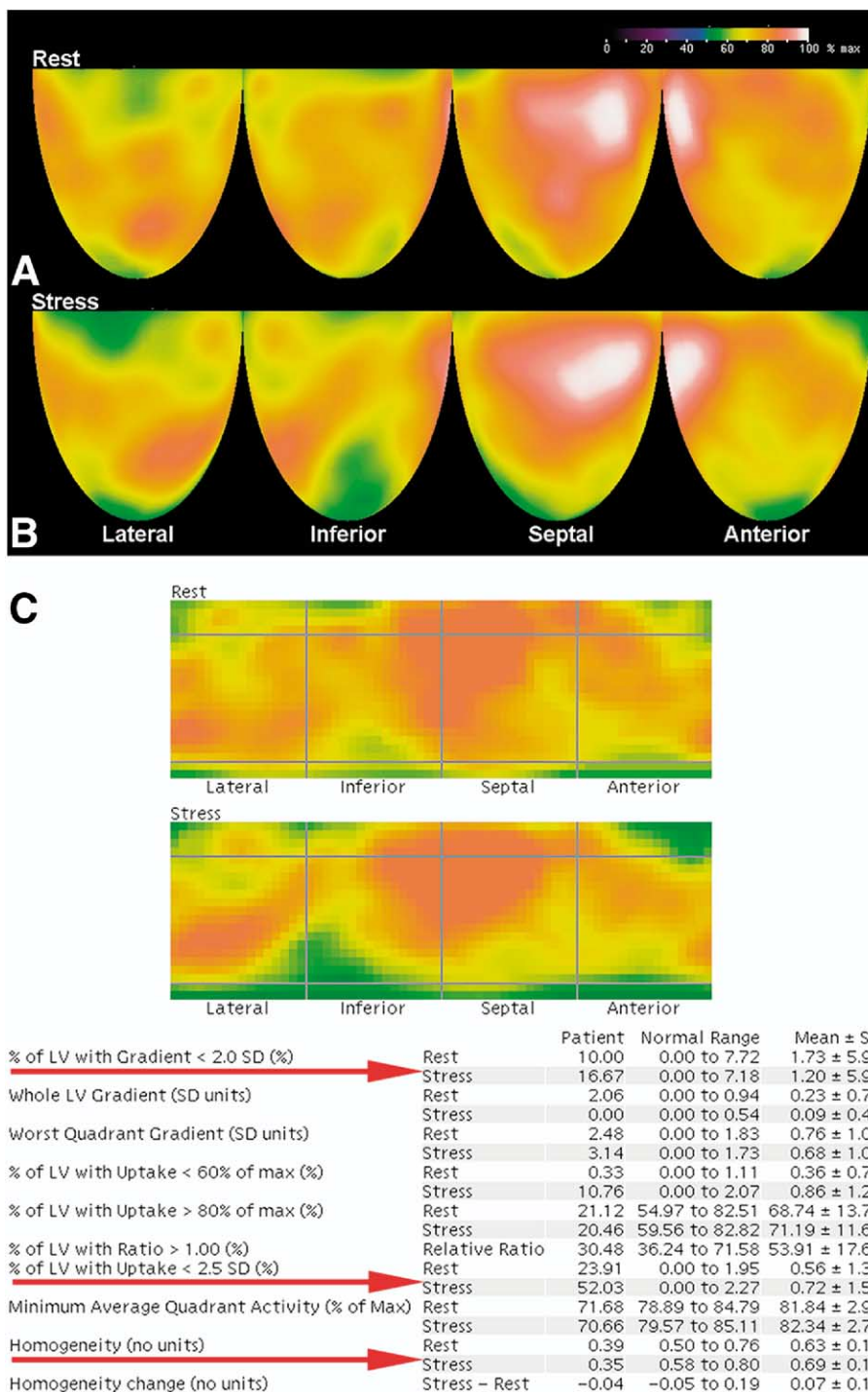
### CLINICAL EXAMPLES OF PERFUSION IMAGES IN EARLY CAD

Figure 5 illustrates PET perfusion images of early coronary atherosclerosis associated with dyslipidemia, elevated triglyceride levels, elevated Lp(a) levels, low HDL levels, and small dense HDL and small dense LDL particle size. The myocardial PET perfusion scans at rest (Figure 5A) and after dipyridamole (Figure 5B) show a base-to-apex longitudinal perfusion gradient and the heterogeneous resting perfusion pattern of endothelial dysfunction characteristic of diffuse coronary atherosclerosis without severe localized stenosis.

The quantitative printout from the baseline rest-stress images (Figure 5C) demonstrates abnormalities of the homogeneity index and the base-to-apex longitudinal perfusion gradient. The square color displays show each quadrant of the heart in a uniform mathematical format of the Markovian homogeneity analysis.<sup>37</sup> Quantitative relative myocardial activity, the base-to-apex longitudinal perfusion gradient, and the homogeneity index are well outside  $\pm 2$  SDs of 50 healthy control subjects.

For the same patient, quantitative comparison of stress images at baseline and at follow-up after 2 years of vigorous lifestyle and pharmacologic treatment (Figure 5D) showed improvement, as did the resting images at baseline compared with follow-up (Figure 5E). The automated software provides objective quantitative measures of all of the possible endpoints immediately for routine clinical comparisons and archives the data so that groups of patients can be followed up for statistical analysis.

Figure 6 demonstrates the earliest abnormality by rest (Figure 6A) and dipyridamole (Figure 6B) perfusion imaging in the absence of any stress-induced perfusion abnormality. The resting perfusion scan shows mild heterogeneity that improved after dipyridamole. The quantitative printout shows that the rest image has an abnormal homogeneity index of 0.38 that is outside  $\pm 2$  SDs of 50 healthy control subjects. After dipyridamole, this homogeneity index improves to 0.62, close to the normal range for stress images. The percent of the left ventricle with activity in the highest range of greater than 80% of maximum increased from 46.7% to 73.7% of the left ventricle, indicating substantial improvement after dipyridamole. There is also an abnormal base-to-apex longitudinal perfusion gradient outside  $\pm 2$  SDs of normal. This patient had hyperhomocysteinemia and dyslipidemia with low HDL levels and small dense LDL and small HDL subtypes. A CT scan showed coronary calcification, and a CT coronary arteriogram showed irregular coronary lumens with minimally



**Figure 5.** Rest (A) and dipyridamole (B) perfusion images of an asymptomatic patient with risk factors showing abnormal perfusion heterogeneity and a base-to-apex longitudinal perfusion gradient. Quantification of severity and a printout of the Markovian homogeneity analysis of baseline images (C) show that 23.9% of the left ventricle (LV) with less than 60% of maximum activity at rest increases to 52% after dipyridamole stress. The homogeneity index is severely abnormal on the resting image, at 0.39, and on the stress image, at 0.35, with normal being 0.63 or above. Quantitative comparison of the baseline stress image to the follow-up stress image (D) shows improvement in the size of the defect from 42% to 9.9% of the left ventricle, which is outside  $\pm 2$  SDs of normal, and a less severe base-to-apex longitudinal perfusion gradient. Quantitative comparison of the baseline rest image to the follow-up rest image (E) shows improvement in the size of the defect from 23.9% to 8.6% of the left ventricle, which is outside  $\pm 2$  SDs of normal; a homogeneity index improving from 0.39 to 0.45; and improvement from 21.1% to 41.8% of the heart having activity in the highest range of greater than 80% of maximum counts.

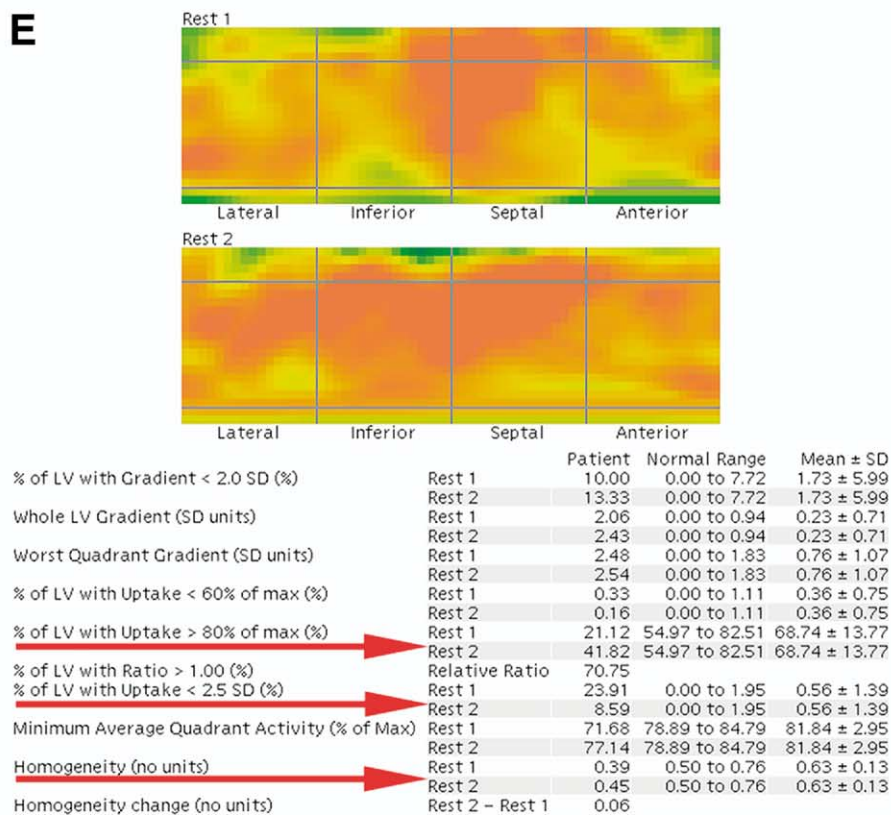
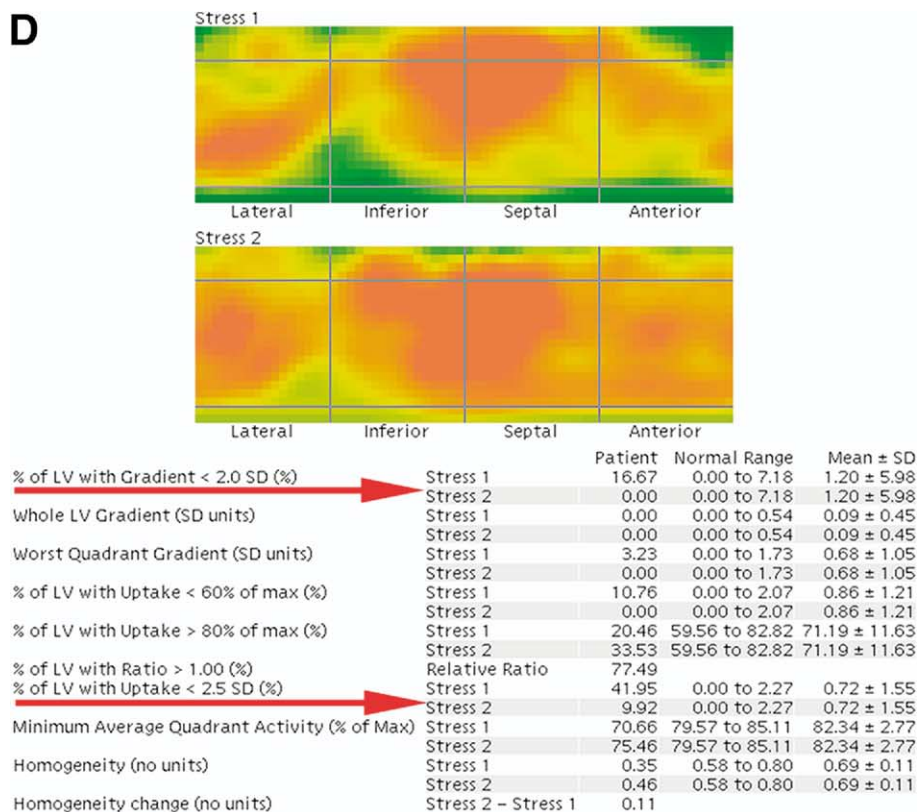
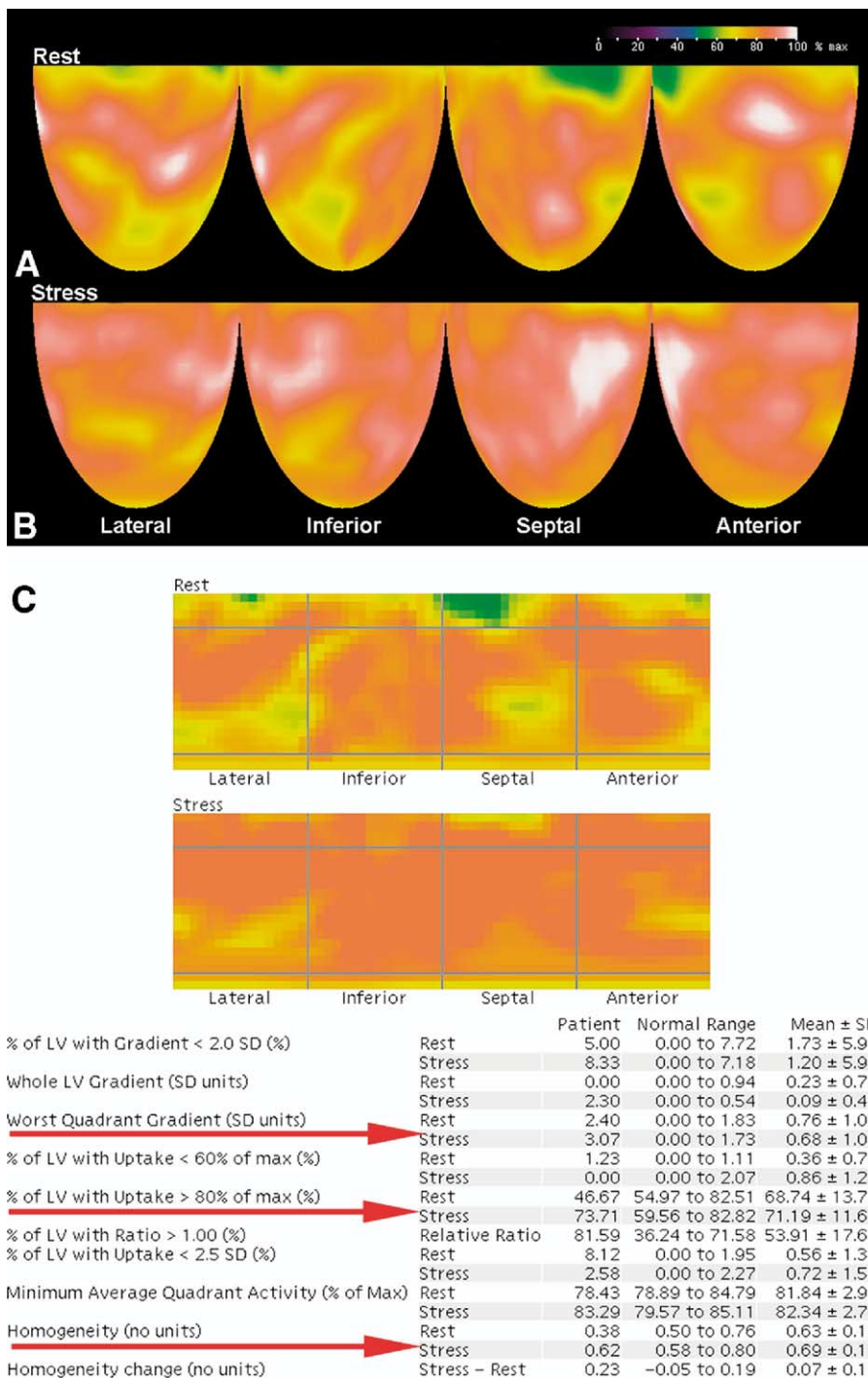


Figure 5. (continued)



**Figure 6.** Rest (A) and dipyridamole (B) images with abnormal heterogeneity of resting perfusion and a mild base-to-apex longitudinal perfusion gradient, both outside  $\pm 2$  SDs of normal with no localized regional defect (C), characteristic of mild diffuse early CAD documented by coronary calcification and noninvasive CT coronary arteriogram.

visible narrowings throughout the coronary arterial tree without significant localized flow-limiting stenosis.

In the Lifestyle Heart Trial,<sup>23</sup> the resting perfusion defects improved, as did the stress perfusion defects,

thereby suggesting that resting perfusion abnormalities due to endothelial dysfunction also improve after treatment, as illustrated in Figure 5 previously and consistent with invasive measures of coronary endothelial dysfunction after

lipid-lowering treatment. In the adenosine sestimibi SPECT postinfarction evaluation (INSPIRE) trial<sup>73</sup> and the clinical outcomes utilizing revascularization and aggressive drug evaluation (COURAGE) trial,<sup>74</sup> changes in resting perfusion defects on follow-up imaging may provide insights on our hypothesis regarding endothelial function, but these studies are not yet completed.

### ABSOLUTE BLOOD FLOW IN MILLILITERS PER MINUTE PER GRAM?

Although objective quantification of relative myocardial perfusion is essential for following changes in CAD, determining absolute myocardial perfusion in milliliters per minute per gram is not, for several reasons<sup>75</sup>: (1) mathematical models for calculating absolute perfusion greatly magnify relative differences in radionuclide uptake into greater differences in absolute perfusion that are subject to substantial errors and greater variability than relative uptake alone; (2) the assumptions inherent in these mathematical models for calculating absolute myocardial perfusion are open to question, which limits clinical reliability; (3) accurate determination of the arterial input function required for models of absolute perfusion is technically difficult and makes PET data acquisition so complex that it causes substantial variability and is rarely used in clinical practice; (4) absolute quantification of myocardial perfusion also requires assumed corrections for partial volume errors that are equally questionable; and (5) quantification of relative myocardial uptake is optimal for changes in CAD without the assumptions and manipulation of the primary data inherent in calculating absolute perfusion.

### CONCLUSIONS AND COMMENT

With current improved PET scanners, recent quantitative software, and cardiac-specific PET technology, definitive studies are now possible to address the role of PET perfusion imaging for early coronary atherosclerosis, for coronary endothelial function, and for their changes during progression or regression as guides to vigorous treatment to prevent, stabilize, or reverse the disease.

High-quality myocardial perfusion imaging provides the basis for nuclear cardiology to achieve a more central role in cardiovascular medicine. Invasive cardiology currently dominates the management of CAD, largely as a result of the integration of diagnostic and therapeutic procedures. Similarly, the nuclear cardiologist may achieve definitive status comparable to the invasive cardiologist by using PET perfusion imaging, as illustrated here, integrated with vigorous short- and long-term clinical management, including definitive decisions regarding revascularization procedures, cardiovascular drugs, aggressive lipid treat-

ment, risk factor control, and intense lifestyle modification, with follow-up in a diagnostic-therapeutic clinical service provided by that nuclear cardiologist.

### Acknowledgment

*The author has indicated he has no financial conflicts of interest.*

### References

1. Brown BG. Familial Atherosclerosis Treatment Study (FATS) 10-year follow-up: triple therapy reduces coronary events [abstract]. *Circulation* 1998;98:1-635.
2. Brown BG, Zhao XQ, Chait A, Fisher LD, Cheung MC, Morse JS, et al. Simvastatin and niacin, antioxidant vitamins, or the combination for the prevention of coronary disease. *N Engl J Med* 2001;345:1583-92.
3. Sdringola S, Nakagawa K, Nakagawa Y, Yusuf SW, Boccalandro F, Mullani N, et al. Combined intense lifestyle and pharmacologic lipid treatment further reduce coronary events and myocardial perfusion abnormalities compared with usual-care cholesterol-lowering drugs in coronary artery disease. *J Am Coll Cardiol* 2003;41:263-72.
4. Hausmann D, Johnson JA, Sudhir K, Mullen WL, Friedrich G, Fitzgerald PJ, et al. Angiographically silent atherosclerosis detected by intravascular ultrasound in patients with familial hypercholesterolemia and familial combined hyperlipidemia: correlation with high density lipoproteins. *J Am Coll Cardiol* 1996;27:1562-70.
5. Raff GL, Gallagher MJ, O'Neill WW, Goldstein JA. Diagnostic accuracy of noninvasive coronary angiography using 64-slice spiral computed tomography. *J Am Coll Cardiol* 2005;46:552-7.
6. Leber AW, Knez A, von Ziegler F, Becker A, Nikolaou K, Paul S, et al. Quantification of obstructive and nonobstructive coronary lesions by 64-slice computed tomography: a comparative study with quantitative coronary angiography and intravascular ultrasound. *J Am Coll Cardiol* 2005;46:147-54.
7. Corti R, Fuster V, Fayad ZA, Worthley SG, Helft G, Chaplin WF, et al. Effects of aggressive versus conventional lipid-lowering therapy by simvastatin on human atherosclerotic lesions: a prospective, randomized, double-blind trial with high-resolution magnetic resonance imaging. *J Am Coll Cardiol* 2005;46:106-12.
8. Kefer J, Coche E, Legros G, Pasquet A, Grandin C, Van Beers BE, et al. Head-to-head comparison of three-dimensional navigator-gated magnetic resonance imaging and 16-slice computed tomography to detect coronary artery stenosis in patients. *J Am Coll Cardiol* 2005;46:92-100.
9. Achenbach S, Daniel WG. Computed tomography of the coronary arteries: more than meets the (angiographic) eye. *J Am Coll Cardiol* 2005;46:155-7.
10. Arad Y, Spadaro LA, Roth M, Newstein D, Guerci AD. Treatment of asymptomatic adults with elevated coronary calcium scores with atorvastatin, vitamin C, and vitamin E: the St. Francis Heart Study randomized clinical trial. *J Am Coll Cardiol* 2005;46:166-72.
11. Gould KL. Pressure-flow characteristics of coronary stenoses in unsedated dogs at rest and during coronary vasodilation. *Circ Res* 1978;43:242-53.
12. Gould KL, Kelley KO, Bolson EL. Experimental validation of quantitative coronary arteriography for determining pressure-flow characteristics of coronary stenosis. *Circulation* 1982;66:930-7.

13. Gould KL, Kirkeeide RL, Buchi M. Coronary flow reserve as a physiologic measure of stenosis severity. *J Am Coll Cardiol* 1990;15:459-74.
14. Seiler C, Kirkeeide RL, Gould KL. Measurement from arteriograms of regional myocardial bed size distal to any point in the coronary vascular tree for assessing anatomic area at risk. *J Am Coll Cardiol* 1993;21:783-97.
15. Seiler C, Kirkeeide RL, Gould KL. Basic structure-function relations of the epicardial coronary vascular tree. Basis of quantitative coronary arteriography for diffuse coronary artery disease. *Circulation* 1992;85:1987-2003.
16. Gould KL, Nakagawa Y, Nakagawa K, Sdringola S, Hess MJ, Haynie M, et al. Frequency and clinical implications of fluid dynamically significant diffuse coronary artery disease manifest as graded, longitudinal, base-to-apex myocardial perfusion abnormalities by noninvasive positron emission tomography. *Circulation* 2000;101:1931-9.
17. De Bruyne B, Hersbach F, Pijls NH, Bartunek J, Bech JW, Heyndrickx GR, et al. Abnormal epicardial coronary resistance in patients with diffuse atherosclerosis but "normal" coronary angiography. *Circulation* 2001;104:2401-6.
18. Schuler G, Hambrecht R, Schlierf G, Grunze M, Methfessel S, Hauer K, et al. Myocardial perfusion and regression of coronary artery disease in patients on a regimen of intensive physical exercise and low fat diet. *J Am Coll Cardiol* 1992;19:34-42.
19. Schuler G, Hambrecht R, Schlierf G, Niebauer J, Hauer K, Neumann J, et al. Regular physical exercise and low-fat diet. Effects on progression of coronary artery disease. *Circulation* 1992;86:1-11.
20. Schwartz RG, Pearson TA, Kalaria VG, Mackin ML, Williford DJ, Awasthi A, et al. Prospective serial evaluation of myocardial perfusion and lipids during the first six months of pravastatin therapy: coronary artery disease regression single photon emission computed tomography monitoring trial. *J Am Coll Cardiol* 2003;42:600-10.
21. Auer J, Berent R, Eber B. Anti-ischemic therapy and myocardial ischemia shown by single photon emission computed tomography imaging. *Circulation* 2001;104:E151-2.
22. Gould KL, Martucci JP, Goldberg DI, Hess MJ, Edens RP, Latifi R, et al. Short-term cholesterol lowering decreases size and severity of perfusion abnormalities by positron emission tomography after dipyridamole in patients with coronary artery disease. A potential noninvasive marker of healing coronary endothelium. *Circulation* 1994;89:1530-8.
23. Gould KL, Ornish D, Scherwitz L, Brown S, Edens RP, Hess MJ, et al. Changes in myocardial perfusion abnormalities by positron emission tomography after long-term, intense risk factor modification. *JAMA* 1995;274:894-901.
24. Czernin J, Barnard RJ, Sun KT, Krivokapich J, Nitzsche E, Dorsey D, et al. Effect of short-term cardiovascular conditioning and low-fat diet on myocardial blood flow and flow reserve. *Circulation* 1995;92:197-204.
25. Yokoyama I, Momomura S, Ohtake T, Yonekura K, Yang W, Kobayakawa N, et al. Improvement of impaired myocardial vasodilatation due to diffuse coronary atherosclerosis in hypercholesterolemics after lipid-lowering therapy. *Circulation* 1999;100:117-22.
26. Bech GJ, De BB, Bonnier HJ, Bartunek J, Wijns W, Peels K, et al. Long-term follow-up after deferral of percutaneous transluminal coronary angioplasty of intermediate stenosis on the basis of coronary pressure measurement. *J Am Coll Cardiol* 1998;31:841-7.
27. Berger A, Botman KJ, MacCarthy PA, Wijns W, Bartunek J, Heyndrickx GR, et al. Long-term clinical outcome after fractional flow reserve-guided percutaneous coronary intervention in patients with multivessel disease. *J Am Coll Cardiol* 2005;46:438-42.
28. Falk E, Shah PK, Fuster V. Coronary plaque disruption. *Circulation* 1995;92:657-71.
29. Brown G, Albers JJ, Fisher LD, Schaefer SM, Lin JT, Kaplan C, et al. Regression of coronary artery disease as a result of intensive lipid-lowering therapy in men with high levels of apolipoprotein B. *N Engl J Med* 1990;323:1289-98.
30. Brown BG, Zhao XQ, Sacco DE, Albers JJ. Atherosclerosis regression, plaque disruption, and cardiovascular events: a rationale for lipid lowering in coronary artery disease. *Annu Rev Med* 1993;44:365-76.
31. Brown BG, Zhao XQ, Sacco DE, Albers JJ. Arteriographic view of treatment to achieve regression of coronary atherosclerosis and to prevent plaque disruption and clinical cardiovascular events. *Br Heart J* 1993;69:S48-53.
32. Mauriello A, Sangiorgi G, Fratoni S, Palmieri G, Bonanno E, Anemona L, et al. Diffuse and active inflammation occurs in both vulnerable and stable plaques of the entire coronary tree: a histopathologic study of patients dying of acute myocardial infarction. *J Am Coll Cardiol* 2005;45:1585-93.
33. Katritsis DG, Ioannidis JP. Percutaneous coronary intervention versus conservative therapy in nonacute coronary artery disease: a meta-analysis. *Circulation* 2005;111:2906-12.
34. Loghini C, Sdringola S, Gould KL. Common artifacts in PET myocardial perfusion images due to attenuation-emission misregistration: clinical significance, causes and solutions in 1177 patients. *J Nucl Med* 2004;45:1029-39.
35. Demer LL, Gould KL, Goldstein RA, Kirkeeide RL, Mullani NA, Smalling RW, et al. Assessment of coronary artery disease severity by positron emission tomography. Comparison with quantitative arteriography in 193 patients. *Circulation* 1989;79:825-35.
36. Nakagawa Y, Nakagawa K, Sdringola S, Mullani N, Gould KL. A precise, three-dimensional atlas of myocardial perfusion correlated with coronary arteriographic anatomy. *J Nucl Cardiol* 2001;8:580-90.
37. Johnson NP, Gould KL. Clinical evaluation of a new concept: resting myocardial perfusion heterogeneity quantified by Markovian analysis of PET identifies coronary microvascular dysfunction and early atherosclerosis in 1034 subjects. *J Nucl Med* 2005;46:1427-37.
38. Quyyumi AA, Dakak N, Andrews NP, Husain S, Arora S, Gilligan DM, et al. Nitric oxide activity in the human coronary circulation. Impact of risk factors for coronary atherosclerosis. *J Clin Invest* 1995;95:1747-55.
39. Casino PR, Kilcoyne CM, Quyyumi AA, Hoeg JM, Panza JA. The role of nitric oxide in endothelium-dependent vasodilation of hypercholesterolemic patients. *Circulation* 1993;88:2541-7.
40. Anderson TJ, Meredith IT, Ganz P, Selwyn AP, Yeung AC. Nitric oxide and nitrovasodilators: similarities, differences and potential interactions. *J Am Coll Cardiol* 1994;24:555-66.
41. Shiode N, Morishima N, Nakayama K, Yamagata T, Matsuura H, Kajiyama G. Flow-mediated vasodilation of human epicardial coronary arteries: effect of inhibition of nitric oxide synthesis. *J Am Coll Cardiol* 1996;27:304-10.
42. Lefroy DC, Crake T, Uren NG, Davies GJ, Maseri A. Effect of inhibition of nitric oxide synthesis on epicardial coronary artery caliber and coronary blood flow in humans. *Circulation* 1993;88:43-54.
43. Sudhir K, MacGregor JS, Amidon TM, Gupta M, Yock PG, Chatterjee K. Differential contribution of nitric oxide to regulation of vascular tone in coronary conductance and resistance arteries: intravascular ultrasound studies. *Am Heart J* 1994;127:858-65.

44. Loscalzo J, Vita JA. Ischemia, hyperemia, exercise, and nitric oxide. Complex physiology and complex molecular adaptations. *Circulation* 1994;90:2556-9.
45. Cohen RA, Vanhoutte PM. Endothelium-dependent hyperpolarization. Beyond nitric oxide and cyclic GMP. *Circulation* 1995;92:3337-49.
46. Schachinger V, Zeiher AM. Quantitative assessment of coronary vasoreactivity in humans in vivo. Importance of baseline vasomotor tone in atherosclerosis. *Circulation* 1995;92:2087-94.
47. Kitakaze M, Node K, Minamino T, Kosaka H, Shinozaki Y, Mori H, et al. Role of nitric oxide in regulation of coronary blood flow during myocardial ischemia in dogs. *J Am Coll Cardiol* 1996;27:1804-12.
48. el-Tamimi H, Mansour M, Wargovich TJ, Hill JA, Kerensky RA, Conti CR, et al. Constrictor and dilator responses to intracoronary acetylcholine in adjacent segments of the same coronary artery in patients with coronary artery disease. Endothelial function revisited. *Circulation* 1994;89:45-51.
49. Penny WF, Rockman H, Long J, Bhargava V, Carrigan K, Ibrham A, et al. Heterogeneity of vasomotor response to acetylcholine along the human coronary artery. *J Am Coll Cardiol* 1995;25:1046-55.
50. Kuo L, Davis MJ, Chilian WM. Longitudinal gradients for endothelium-dependent and -independent vascular responses in the coronary microcirculation. *Circulation* 1995;92:518-25.
51. Chilian WM, Dellspurger KC, Layne SM, Eastham CL, Armstrong MA, Marcus ML, et al. Effects of atherosclerosis on the coronary microcirculation. *Am J Physiol* 1990;258:H529-39.
52. Sellke FW, Armstrong ML, Harrison DG. Endothelium-dependent vascular relaxation is abnormal in the coronary microcirculation of atherosclerotic primates. *Circulation* 1990;81:1586-93.
53. Kuo L, Davis MJ, Cannon MS, Chilian WM. Pathophysiological consequences of atherosclerosis extend into the coronary microcirculation. Restoration of endothelium-dependent responses by L-arginine. *Circ Res* 1992;70:465-76.
54. Zeiher AM, Drexler H, Wollschlager H, Just H. Endothelial dysfunction of the coronary microvasculature is associated with coronary blood flow regulation in patients with early atherosclerosis. *Circulation* 1991;84:1984-92.
55. Zeiher AM, Drexler H, Wollschlager H, Just H. Modulation of coronary vasomotor tone in humans. Progressive endothelial dysfunction with different early stages of coronary atherosclerosis. *Circulation* 1991;83:391-401.
56. Zeiher AM, Krause T, Schachinger V, Minners J, Moser E. Impaired endothelium-dependent vasodilation of coronary resistance vessels is associated with exercise-induced myocardial ischemia. *Circulation* 1995;91:2345-52.
57. Verma S, Anderson TJ. Fundamentals of endothelial function for the clinical cardiologist. *Circulation* 2002;105:546-9.
58. Clarkson P, Celermajer DS, Powe AJ, Donald AE, Henry RM, Deanfield JE. Endothelium-dependent dilatation is impaired in young healthy subjects with a family history of premature coronary disease. *Circulation* 1997;96:3378-83.
59. Suwaidi JA, Hamasaki S, Higano ST, Nishimura RA, Holmes DRJ, Lerman A. Long-term follow-up of patients with mild coronary artery disease and endothelial dysfunction. *Circulation* 2000;101:948-54.
60. Schachinger V, Britten MB, Zeiher AM. Prognostic impact of coronary vasodilator dysfunction on adverse long-term outcome of coronary heart disease. *Circulation* 2000;101:1899-906.
61. Halcox JP, Schenke WH, Zalos G, Mincemoyer R, Prasad A, Waclawiw MA, et al. Prognostic value of coronary vascular endothelial dysfunction. *Circulation* 2002;106:653-8.
62. Bugiardini R, Manfrini O, Pizzi C, Fontana F, Morgagni G. Endothelial function predicts future development of coronary artery disease: a study of women with chest pain and normal coronary angiograms. *Circulation* 2004;109:2518-23.
63. Nesto RW, Lamas GA, Barry J. Paradoxical elevation of threshold to angina pectoris by cold pressor test in men with significant coronary artery disease. *Am J Cardiol* 1989;63:656-9.
64. Kjaer A, Meyer C, Nielsen FS, Parving HH, Hesse B. Dipyridamole, cold pressor test, and demonstration of endothelial dysfunction: a PET study of myocardial perfusion in diabetes. *J Nucl Med* 2003;44:19-23.
65. Gould KL, Lipscomb K, Hamilton GW. Physiologic basis for assessing critical coronary stenosis. Instantaneous flow response and regional distribution during coronary hyperemia as measures of coronary flow reserve. *Am J Cardiol* 1974;33:87-94.
66. Gould KL. Noninvasive assessment of coronary stenoses by myocardial perfusion imaging during pharmacologic coronary vasodilatation. I. Physiologic basis and experimental validation. *Am J Cardiol* 1978;41:267-78.
67. Gould KL, Schelbert HR, Phelps ME, Hoffman EJ. Noninvasive assessment of coronary stenoses with myocardial perfusion imaging during pharmacologic coronary vasodilatation. V. Detection of 47 percent diameter coronary stenosis with intravenous nitrogen-13 ammonia and emission-computed tomography in intact dogs. *Am J Cardiol* 1979;43:200-8.
68. Gould KL, Goldstein RA, Mullani NA, Kirkeeide RL, Wong WH, Tewson TJ, et al. Noninvasive assessment of coronary stenoses by myocardial perfusion imaging during pharmacologic coronary vasodilatation. VIII. Clinical feasibility of positron cardiac imaging without a cyclotron using generator-produced rubidium-82. *J Am Coll Cardiol* 1986;7:775-89.
69. Gould KL. Coronary artery stenosis and reversing atherosclerosis. 2nd ed. London: Arnold Publishers; 1999.
70. Doudkine A, Macaulay C, Poulin N, Palcic B. Nuclear texture measurements in image cytometry. *Pathologica* 1995;87:286-99.
71. King RB, Bassingthwaight JB, Hales JR, Rowell LB. Stability of heterogeneity of myocardial blood flow in normal awake baboons. *Circ Res* 1985;57:285-95.
72. Bassingthwaight JB, King RB, Roger SA. Fractal nature of regional myocardial blood flow heterogeneity. *Circ Res* 1989;65:578-90.
73. Mahmarian JJ, Shaw LJ, Olszewski GH, Pounds BK, Frias ME, Pratt CM. Adenosine sestamibi SPECT post-infarction evaluation (INSPIRE) trial: a randomized, prospective multicenter trial evaluating the role of adenosine Tc-99m sestamibi SPECT for assessing risk and therapeutic outcomes in survivors of acute myocardial infarction. *J Nucl Cardiol* 2004;11:458-69.
74. Chiquette E, Chilton R. Aggressive medical management of coronary artery disease versus mechanical revascularization. *Curr Atheroscler Rep* 2003;5:118-23.
75. Yoshida K, Mullani N, Gould KL. Coronary flow and flow reserve by PET simplified for clinical applications using rubidium-82 or nitrogen-13-ammonia. *J Nucl Med* 1996;37:1701-12.